7 *Ozone Response to Precursor Controls in Very Complex Terrains: Use of Photochemical Indicators to Assess O_3-NO_x-VOCs Sensitivity in the Northeastern Iberian Peninsula*

Published as Jiménez, P., Baldasano, J.M., 2004. Ozone response to precursor controls in very complex terrains: Use of photochemical indicators to assess O_3-NO_x-VOC sensitivity in the northeastern Iberian Peninsula. Journal of Geophysical Research, ***109****, D20309, doi: 10.1029/2004JD004985.*

7.1 Introduction

The kinetics of ozone (O_3) chemistry and its two main precursors, nitrogen oxides (NO_x) and volatile organic compounds (VOCs) represents an important field of uncertainty in atmospheric chemistry and photochemical modeling (Atkinson, 2000). It is generally known that under some conditions, O_3 concentrations increase with increasing NO_x and are largely insensitive to VOCs, while for other conditions the rate of formation will increase with increasing VOCs and will be unchanged or decrease with increasing NO_x. This complexity affects the design of control strategies to reduce tropospheric O_3 production, and considerable interest exists in finding observable indicators of how real air masses are likely to respond to emission controls. A major problem for the study of O_3-NO_x-VOCs sensitivity has been the inability to gain evidence based on direct measurements rather than theoretical calculations (Sillman, 1999). This problem has been especially critical when different models have given contradictory results on the effectiveness of NO_x versus VOCs control.

Milford *et al.* (1994) developed an approach for evaluating NO_x-VOCs sensitivity. They found that model predictions for NO_x-VOCs sensitivity were linked to simulated concentrations of a number of key species. VOC-sensitive ozone in models is associated with afternoon values of total reactive nitrogen (NO_y) above a certain threshold concentration, while NO_x-sensitivity ozone was associated with lower NO_y. Sillman (1995) and Sillman *et al.* (1998) extended the work of Milford *et al.* (1994) in order to include other indicator species and ratios: O_3/NO_y, O_3/NO_z (where NO_z is defined as NO_y-NO_x), and H_2O_2/HNO_3. In recent years, a number of works have deepened in the analysis of photochemical indicators that determine the split into VOC-sensitive and NO_x-sensitive regimes (Tonnesen and Dennis, 2000a, 2000b; Blanchard and Stoeckenius, 2001; Blanchard and Fairley, 2001; Sillman and He, 2002; Sillman *et al.*, 2003; among others). Nevertheless, it is still unclear whether the indicator ratios would show similar behavior for a wide variety of conditions.

Blanchard *et al.* (1999) and Blanchard and Stoeckenius (2001) used the extent of reaction parameter (EOR) to describe how far a system has proceeded towards its maximum possible O_3 production, with the transition from radical- to NO_x-limitation typically occurring when the extent of reaction is 0.9 (dimensionless units). EOR was derived from smog chamber experiments and is based on the finding that O_3 in photochemically aged air is sensitive to NO_x while air with relatively unprocessed emissions is sensitive to VOCs. Box-model and three-dimensional model simulations indicate that when the extent of reaction remains below ~0.6 during the hours of peak ozone, O_3 formation is limited by the availability of radicals, rather than NO_x, and O_3 concentrations respond to changes in VOCs levels (Blanchard and Fairley, 2001).

Here we show results from model calculations that relate NO_x-VOCs sensitivity in as very complex an area as the northeastern Iberian Peninsula. We use a three-dimensional air quality model (MM5-EMICAT2000-CMAQ) to represent O_3 formation and transport. A series of scenarios are analyzed in order to establish their chemical regime. Using the model to study three different scenarios gives the opportunity to compare the variation of indicator values in each zone and to check whether O_3 values react consistently to similar changes in emissions. Correlations between model species concentrations and NO_x-VOCs sensitivity predictions are examined to see whether commonly employed indicators can be correlated with NO_x-VOCs sensitivity in the case of northeastern Iberian Peninsula. This O_3 sensitivity analysis provides an evaluation of NO_x and VOCs hypothetical control policies through a comparison of simulated correlation between the species.

7.2 The Use of Indicator Species

The split between NO_x-sensitive and VOC-sensitive conditions is well known. For conditions with relatively high VOCs and low NO_x, O_3 increases with increasing NO_x and is relatively insensitive to changes in VOCs. For conditions with relatively low VOCs and high NO_x, O_3 increases with increasing VOCs and decreases with increasing NO_x. An analogous split between "NO_x-sensitive" and "NO_x-saturated" regimes occurs in the remote troposphere, although for remote conditions O_3 increases with increasing VOCs even in the NO_x-sensitive regime (Sillman and He, 2002). These phenomena are driven by the complex ozone chemistry.

The split between NO_x-sensitive and VOC-sensitive regimes is driven by the chemistry of odd hydrogen radicals. The NO_x-VOCs split is attributed to the relative rate of formation of peroxides (via HO_2-HO_2 and HO_2-RO_2 reactions) relative to nitric acid formation (via reaction OH + NO_2). NO_x-sensitive conditions occur when peroxides dominate over nitric acid as radical sinks, while NO_x-saturated conditions occur when nitric acid dominates (Sillman, 1999).

NO_x-VOCs sensitivity is attributed to the relative source strengths of odd hydrogen radicals (S_H) and odd nitrogen (S_N), summed over the period of O_3 production for an air parcel (Sillman and

He, 2002). VOC-sensitive chemistry occurs when the odd nitrogen source exceeds the source of odd hydrogen. According to Kleinman *et al.* (1997), the instantaneous rate of O_3 production is VOC-sensitive whenever the instantaneous loss rate for odd nitrogen (L_N) is greater then half of the total odd hydrogen source ($L_N/Q > 0.5$). Odd hydrogen sources must be in steady state with its three major sinks (equation 7.1):

$$S_H = 2P_{perox} + P_{HNO3} + P_{PANS} \quad (7.1)$$

where P_{perox} and P_{HNO3} represent production rates for peroxides (including H_2O_2 and organic peroxides) and HNO_3, and P_{PANS} represents net photochemical production of peroxyacetyl nitrate (PAN) and higher order analogues. VOC-sensitive chemistry would occur whenever P_{HNO3} exceeds $2P_{perox}$. The NO_x-VOC split is mainly associated with formation of nitric acid but is not greatly affected by formation of PAN. Sensitivity transition from NO_x-sensitive to VOC-sensitive conditions can be defined in equation 7.2 (Sillman and He, 2002):

$$\frac{1}{Q_N}\frac{\partial[O_3]}{\partial Q_N} = \frac{1}{Q_H}\frac{\partial[O_3]}{\partial Q_H} \quad (7.2)$$

where $[O_3]$ represents ozone concentrations and Q_N and Q_H represent emission rates for NO_x and VOCs. Using this definition, the sensitivity transition represents the point at which a given percent reduction in either NO_x or VOC would result in the same reduction in ozone.

Tonnesen and Dennis (2000a) analyzed O_3 formation in terms of radical formation equivalent, radical termination (through production of peroxides, HNO_3 and organic nitrates) and radical propagation, finding out that production rate for O_3 is proportional to the rate of the VOCs + OH reactions. Sillman (1995) suggested that O_3 was roughly proportional to the odd hydrogen source, being the ratio O_3/NO_z analogous to the quotient S_H/L_N, which is related to NO_x-VOC sensitivity. Following this basis, Sillman (1995) proposed some indicators including O_3/NO_y, O_3/NO_z, O_3/HNO_3, H_2O_2/HNO_3, H_2O_2/NO_z and the equivalent ratios with summed H_2O_2 and organic peroxides.

7.3 Methods

Modeling results are based the photochemical pollution event in the Western Mediterranean Basin that took place on 13-16 August, 2000 (see Section 2.1). Simulations with MM5-EMICAT2000-CMAQ show the results for 14 August, 2000, at 1200UTC, the hour of maximum simulated ground-level O_3 production. This is a representative day of this episode for the domain of study of the northeastern Iberian Peninsula. The effect of controlling ozone precursors on sensitivity regimes was evaluated performing simulations for the domain with baseline emission rates for VOCs and NO_x as derived from EMICAT2000 model, and reducing anthropogenic VOCs and NO_x emissions on a 35% following the methods by Milford *et al.* (1994), Sillman (1995) and

Sillman *et al.* (2003). Meteorology represents the same day in order not to introduce any external influence. Three inner scenarios were deeply analyzed: (a) a 32 x 32 km^2 urban area centered in the city of Barcelona that comprises the Barcelona Geographical Area (BGA); (b) a 32 x 32 km^2 background area centered in Plana de Vic (VIC); and (c) a 32 x 32 km^2 industrial zone centered in Alcover (ALC). The selection of these scenarios is based in the important photochemical pollution episodes in the northeastern Iberian Peninsula.

The peculiar topography of the zone is the principal driving mechanism that contributes to the dispersion of emissions in the given domain. Maximum O_3 levels in the northeastern Iberian Peninsula are measured in Plana de Vic and Alcover industrial zone (over 80 ppb). As derived from simulations (Figure 7.1), air masses from Barcelona Geographical Area are advected to the zone of Plana de Vic through river valley canalizations, transporting ozone precursors. These air masses departing from Barcelona act as photochemical reactors as they move northeast (the component of the wind is south-southwest) until they reach the region of Vic. Alcover high O_3 levels have a local origin according to the high weight of heavy-chemical industry in the area.

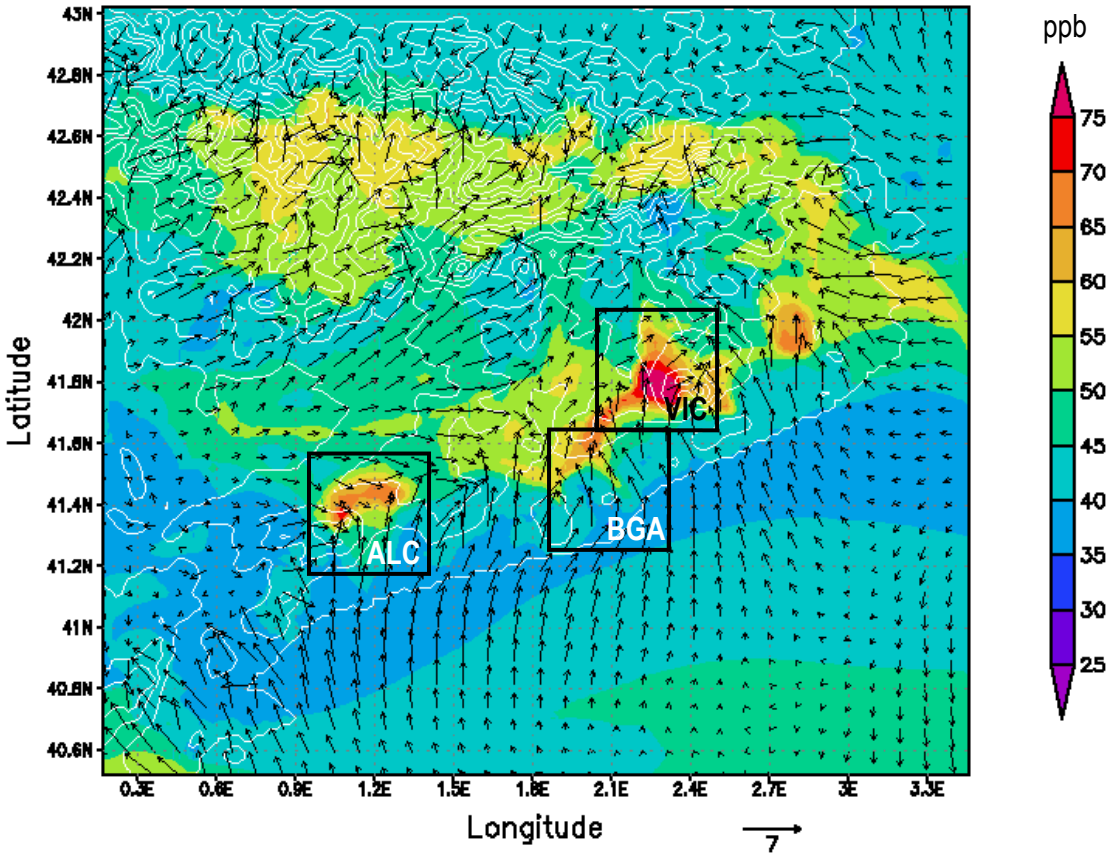

Figure 7.1. Surface ozone concentration (ppb) and wind fields (m s^{-1}) at 1200UTC of 14 August, 2000, in the northeastern Iberian Peninsula, as simulated by MM5-EMICAT2000-CMAQ air quality model.

Hourly measures of ground-level O_3 simulation results in each case and scenario were compared with the measurements from 48 air quality surface stations in northeastern Spain (Catalonia), which belong to the Environmental Department of the Catalonia Government and are located within the above scenarios. The non-availability of measurements of other pollutants with an interest as indicators (e.g. NO_y, H_2O_2 or HNO_3) leads us to focus on the evaluation of ground-level O_3. Statistical discrete parameters (UPA, MNBE, MNGE) set by US EPA (1991), as described in Chapter 5 of this document, were utilized to establish the performance of the model.

The analysis of the results will consist of a statistical evaluation, comparing the first-layer simulations results and the values measured in the air quality stations of the domain under study. Meteorological model has also been evaluated comparing model results with surface and aloft wind measurements. Validation data of 52 surface stations located across the domain, and a radiosonde launched in Barcelona (in the center of the domain in the coast) were used.

7.4 Response to NO_x and VOCs Controls

The correspondence between NO_x-VOCs sensitivity and indicator values can be examined in greater detail if quantitative methods are used to define NO_x-VOCs chemistry. For these purposes, we could use the definition by Sillman *et al.* (2003). Locations are defined as NO_x-sensitive for a specified hour if O_3 in the case with 35% reduced NO_x is lower than O_3 in both the base case and in the case with 35% reduced VOCs by at least 2 ppb. Locations are classified as VOC-sensitive if the O_3 in the case with reduced VOCs is lower than O_3 in the other cases by at least 2 ppb. Locations that are neither VOC-sensitive of NO_x-sensitive by this definition are classified as having mixed sensitivity if O_3 in the cases with the reduced NO_x and with reduced VOCs is lower than O_3 in the base case by at least 2 ppb; locations are classified as insensitive to NO_x and VOCs otherwise. These definitions are time-dependent; that is, a model location may be NO_x-sensitive at some times and VOC-sensitive at other times. Lu and Chang (1998) used another definition, which separates extreme cases, that is, locations where only NO_x or only VOCs controls are effective. Their definition is based on zero lines of simulated reduction in peak O_3 associated with reduced NO_x, versus reduction associated with reduced VOCs (Andreani-Aksoyoglu *et al.*, 2001).

A preliminary examination of geographic patterns of responses to emission reductions at 1200UTC shows that the area with the most elevated O_3 concentration (VIC), benefits from NO_x reductions (reduction of 10 ppb in ground-level O_3 levels), meanwhile the same reduction emissions causes an important increment of O_3 in the city of Barcelona (9 ppb) and downwind the industrial area of Tarragona (18 ppb) (Figure 7.2a). Cities located in BGA and the plume departing from the city of Barcelona benefit form VOCs reductions (10 ppb of O_3), as well as the industrial zone of ALC (20 ppb) (Figure 7.2b). The rest of the domain is practically insensitive to VOCs reductions. This behavior is more clearly seen when studying differences between O_3 levels in the case of 35% VOC reduction and 35% NO_x reduction (Figure 7.2c).

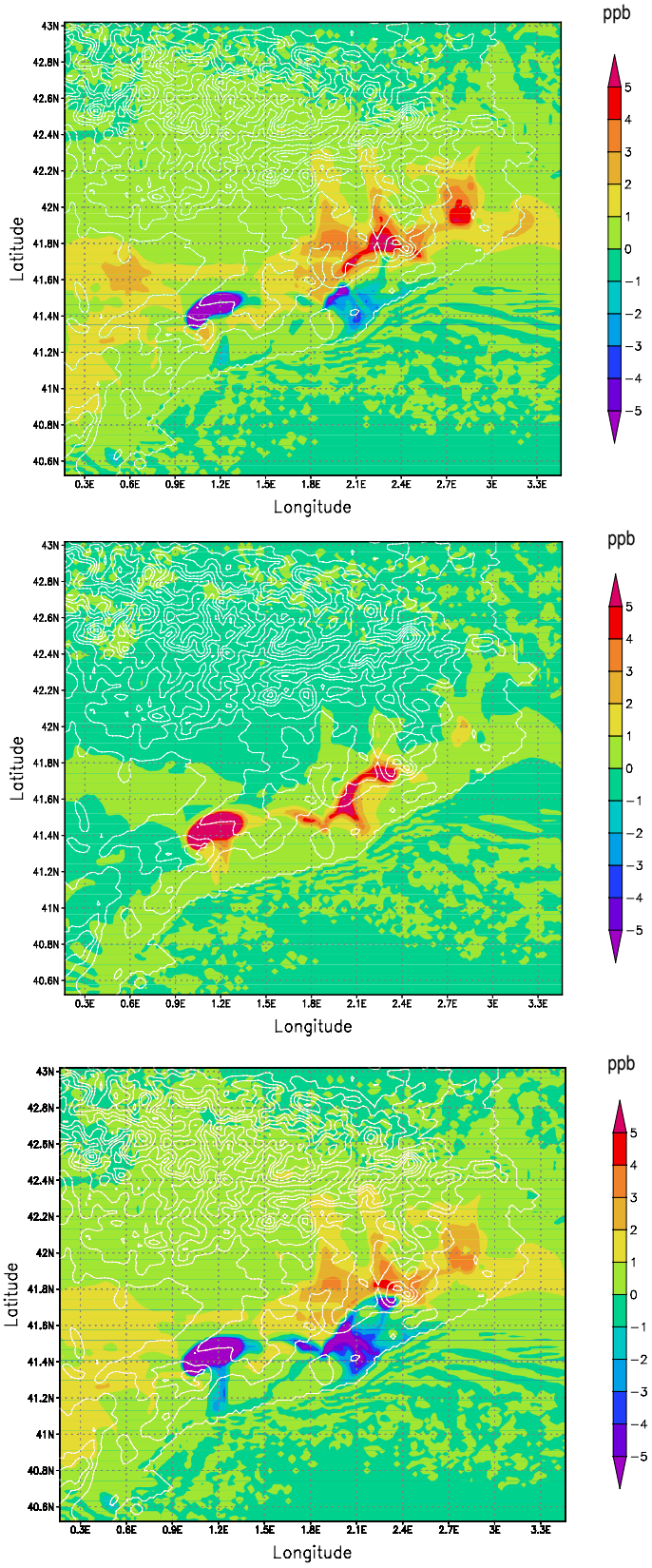

Figure 7.2. Reduction in peak ozone concentrations (ppb) at 1200UTC due to; (a) 35% reduction in NO_x emissions (Base case – NO_x reduction case); (b) 35% reduction in VOCs emissions (Base case – VOCs reduction case); and (c) difference between VOCs reduction case – NO_x reduction case.

Figure 7.3a illustrates the distribution of the cells of the domain according to their NO_x- or VOC-sensitivity using Sillman *et al.* (2003) definition, derived from BGA, VIC and ALC scenarios. This definition indicates locations where NO_x or VOCs controls are more effective in reducing O_3 production. As derived from this definition, most cells in BGA and ALC are under a VOC-sensitive regime or have a mixed sensitivity; meanwhile VIC is dominated by NO_x-sensitive chemistry.

According to the criterion of Lu and Chang (1998), the grid cells in the top-left quadrant of Figure 7.3b are characterized with NO_x-sensitive chemistry. They show considerable O_3 decrease with decreasing NO_x, and insignificant O_3 reduction when reducing VOCs. This approach assumes that the grid cells in the top-right quadrant are sensitive to both VOCs and NO_x controls. Grid cells in the bottom-right quadrant, where O_3 diminishes with decreasing VOCs but increases with decreasing NO_x, are referred to as VOC-sensitive grid cells. The bottom-left quadrant is empty. According to this definition, most of the grid cells in BGA are VOC-sensitive, meanwhile cells in VIC have a mixed sensitivity. The domain of ALC is NO_x- and VOC-sensitive for several cells; meanwhile most of the domain presents a VOC-limited regime.

7.4.1 Model-Measurement Comparisons

Despite that a surface measurement represents a value only at a given horizontal location and height, while the concentration predicted by the model represents a volume-averaged value, comparisons of model and measured variables represents a useful tool to depict the behavior of every case in the scenarios considered.

Table 7.1 shows the root mean square error (RMSE) of wind speed at 10m, for the lower, middle and upper troposphere and RMSE of wind direction (10 m) at 0000, 1200 and 2400UTC. The general behavior of the model shows a tendency to overestimate nocturnal surface winds and to underestimate the diurnal flow. A clear improvement is produced in the simulation during the central part of the day; at this time, the complex structure of the see-breeze described by simulation and the development of up-slope winds appears to agree in a higher grade with surface measurements. The statistics show how the model presents a better behavior within the boundary layer, and major disagreement with the radiosonde appears over 1000m above ground level.

Although there is no objective criterion set forth for a satisfactory model performance in the case of ozone, suggested values of ±10–15% for MNBE, ±15–20% for the UPA and +30–35% for the MNGE to be met by modeling simulations of O_3 have been considered for regulatory applications (Russell and Dennis, 2000; Hogrefe *et al.*, 2001).

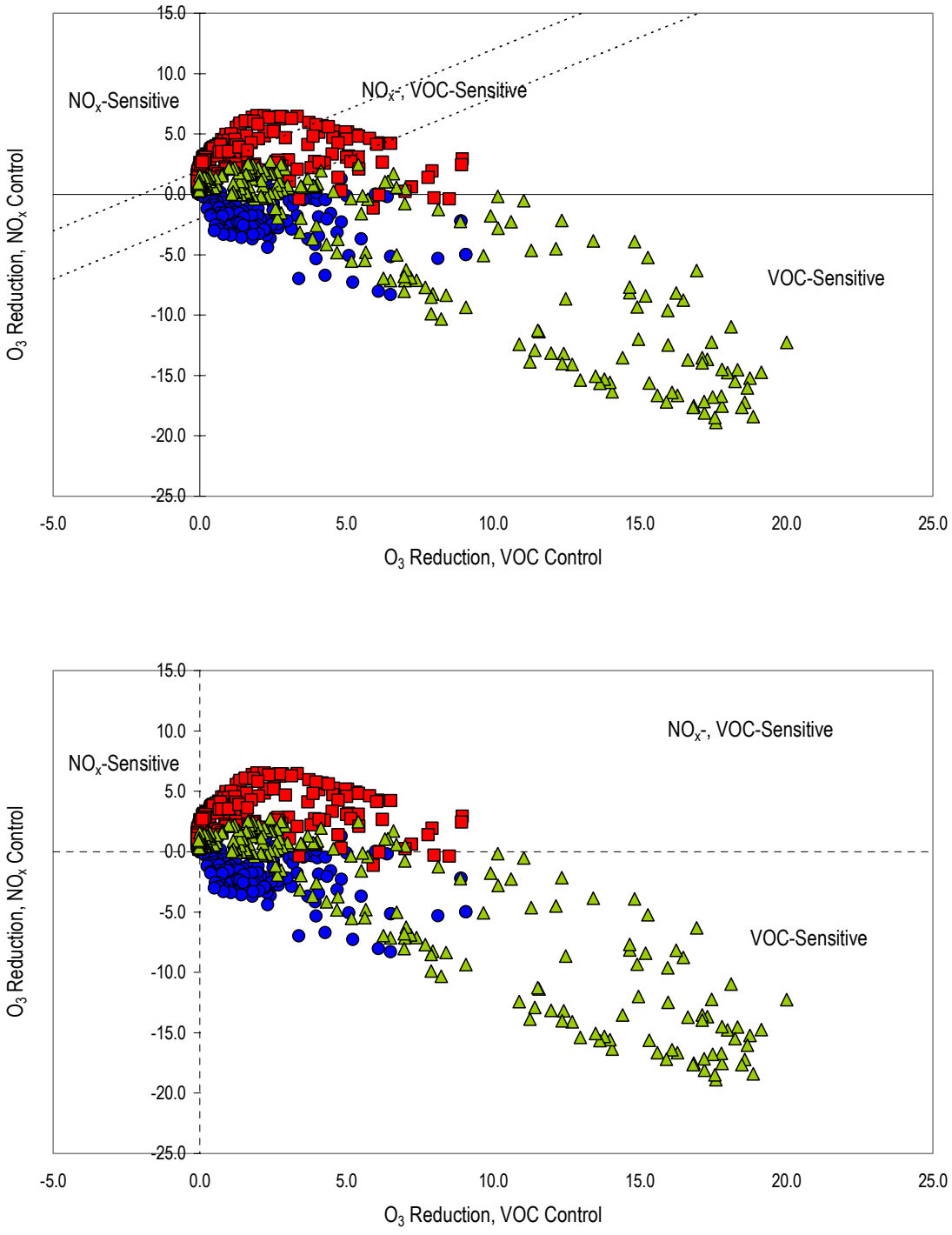

Figure 7.3. Relation between ozone reductions due to NO_x controls (35% emission reduction) and VOC controls (35% emission reduction) for Barcelona Geographical Area (circles), Plana de Vic (squares) and Alcover (triangles) using (a) the definition of Sillman *et al.* (2003); and (b) the definition of Lu and Chang (1998).

Table 7.1. RMSE statistic of wind speed, and wind direction at 0000UTC, 1200UTC and 2400UTC for 14 August, 2000 (surface values evaluated with 52 surface stations, aloft values evaluated with a radiosonde).

RMSE Wind speed (m/s)			
	0000UTC	***1200UTC***	***2400UTC***
Surface 10 m	1.71	2.04	2.00
Radiosonde <1000 m	0.84	1.04	1.31
1000-5000 m	5.03	1.55	3.7
5000-10000 m	8.45	5.15	3.94
RMSE Wind direction (º)			
	0000UTC	***1200UTC***	***2400UTC***
Surface 10 m	95.95	44.74	89.40

Figure 7.4 and Table 7.2 show the results of the evaluation of ground-level O_3. Peak O_3 in the different scenarios is slightly lower than the measured values for each considered case. Comparison between model and measurements shows a good agreement when the model predicts dominant VOC-sensitive chemistry in the BGA and ALC scenarios. Here, statistical parameters of O_3 evaluation get worse when reducing VOCs emissions and improve in the –35% NO_x case, specially in the Barcelona Geographical Area, where UPA reduces from –18% in the VOC-reduction case until –8% in the NO_x-reduction case). The same behavior is observed in Alcover. By contrast, the evaluation in VIC depicts a clear underprediction of O_3 levels (around –18% of MNBE, 27% of MNGE and –13% of UPA).

Statistic parameters in the stations of Plana de Vic worsen when reducing precursor emissions on a 35%, especially in the case of 35% NO_x reduction, which yields to a more important underestimation of O_3 levels in the area because of the NO_x-limited regime of this scenario. It is noteworthy that all model cases meet the criteria established by US EPA for model evaluations in the case of O_3.

Model-measurement comparison suggests that the O_3-production chemistry may not be sufficiently reactive, possibly because of an underestimation in reactive VOCs and/or an overestimation in NO_x emissions. The inferior bias compared to the observations of air quality stations for the cells in ALC and BGA may be due to the pervasive emissions in the near-source cells and therefore emissions strength better fits measurements. Differences in the O_3 concentrations between model and measurements are higher in the domain of VIC. This may be due because the photochemical O_3 production is subdued in background cells, being most of the O_3 transported from the BGA-departing plume; and hence, the relative contribution from the different emissions is not as significant as in the urban or industrial cells.

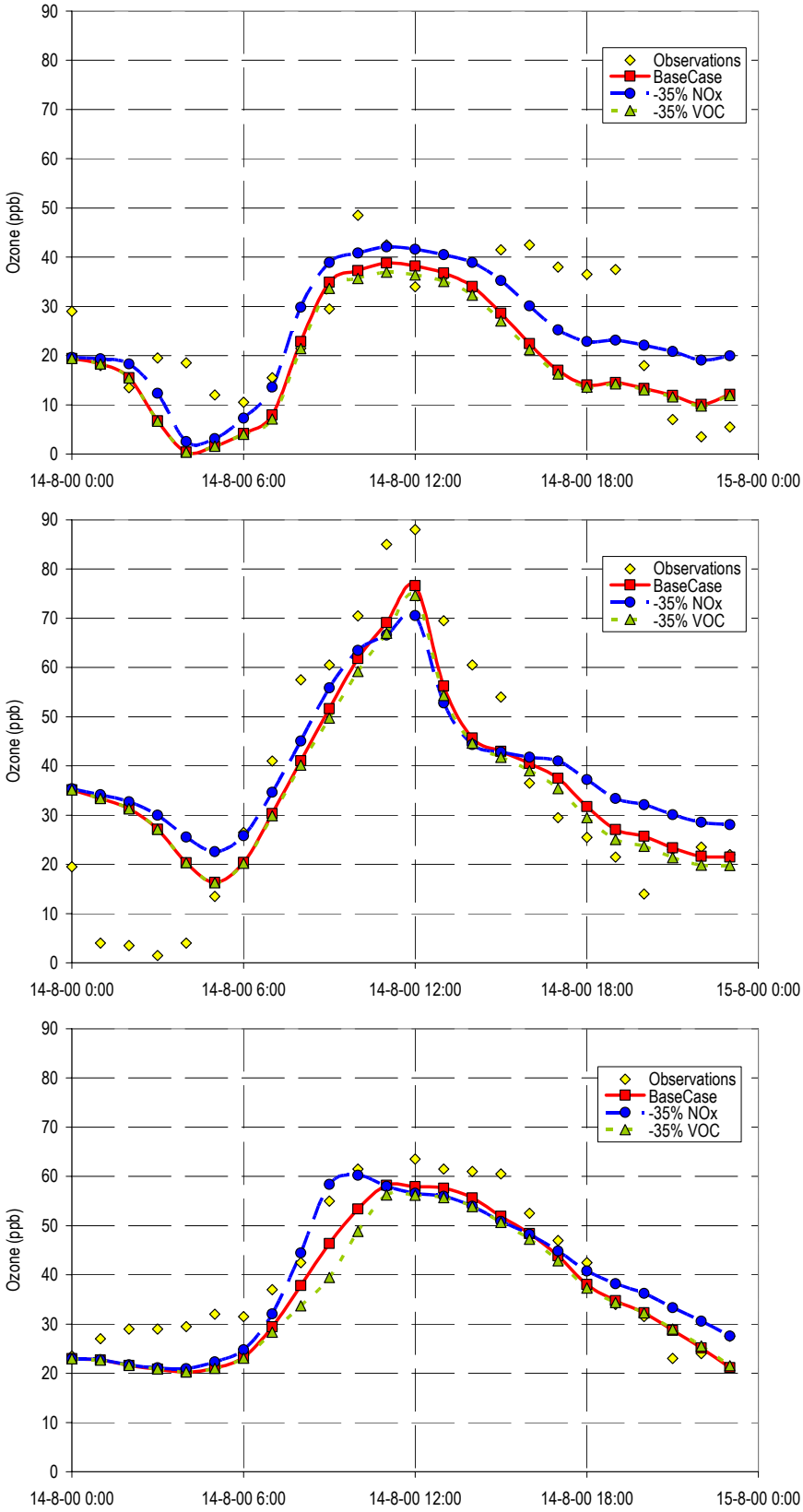

Figure 7.4. Measured O_3 (diamonds) versus modeled O_3 for August 14, 2000, for the base case (solid line, squares), 35% NO_x reduction case (dashed, circles) and the 35% VOCs reduction case (dashed, triangles) in stations of (a) Barcelona (BGA); (b) Vic; and (c) Alcover. Statistics are shown in Table 7.2.

Table 7.2. Evaluation of ozone concentrations for 14 August, 2000, according to the scenario: mean normalized bias error (MNBE), mean normalized gross error (MNGE) and unpaired peak accuracy (UPA).

Barcelona Geographical Area (Urban)			
Max Measured (ppb)		49	
	Base Case	***-35% NO_x***	***-35% VOC***
Max Simulated (ppb)	42	45	40
MNBE (%)	-17.31	-10.16	-19.36
MNGE (%)	24.11	23.76	28.16
UPA (%)	-13.56	-7.94	-17.52
Plana de Vic (Background)			
Max Measured (ppb)		88	
	Base Case	***-35% NO_x***	***-35% VOC***
Max Simulated (ppb)	77	71	75
MNBE (%)	-18.64	-19.69	-22.02
MNGE (%)	27.62	31.16	28.39
UPA (%)	-12.90	-19.84	-15.14
Alcover (Industrial)			
Max Measured (ppb)		64	
	Base Case	***-35% NO_x***	***-35% VOC***
Max Simulated (ppb)	58	60	56
MNBE (%)	-14.07	-11.75	-15.68
MNGE (%)	19.58	19.31	20.20
UPA (%)	-8.31	-5.12	-11.47

Despite these differences, the link between NO_x-VOC sensitivity and photochemical indicators is largely unaffected by changes in model assumptions, including assumed emission rates for both anthropogenic and biogenic species (Sillman *et al.*, 1998).

7.4.2 Use of Photochemical Indicators

NO_y. NO_y works as an indicator because it is related to the balance between VOCs and NO_x seen by an air mass. In addition, the association of ozone sensitivity with NO_y reflects a feature of photochemical evolution that is independent of initial VOCs/NO_x ratios (Milford *et al.*, 1994). Figure 7.5 shows reductions in peak O_3 associated with 35% reductions in anthropogenic VOCs and NO_x emissions, plotted against the base case NO_y concentration predicted for the grid cells at 1200UTC. Reductions in VOCs have little impact on peak O_3 in locations where NO_y is low, but as NO_y increases, the reduction in O_3 associated with reduced VOCs increases in an approximately log-linear way. In all cases, a crossover occurs at 4 ppb NO_y, where reductions in VOCs become more effective than reductions in NO_x. For the BGA and ALC scenarios, Figures 7.5a and 7.5c show a sharp delineation between VOC-sensitive (corresponding to NO_y concentrations above 4 ppb) and NO_x-sensitive locations (concentrations under this threshold). The overlap between NO_x- and VOC-sensitive locations occupies a very narrow range.

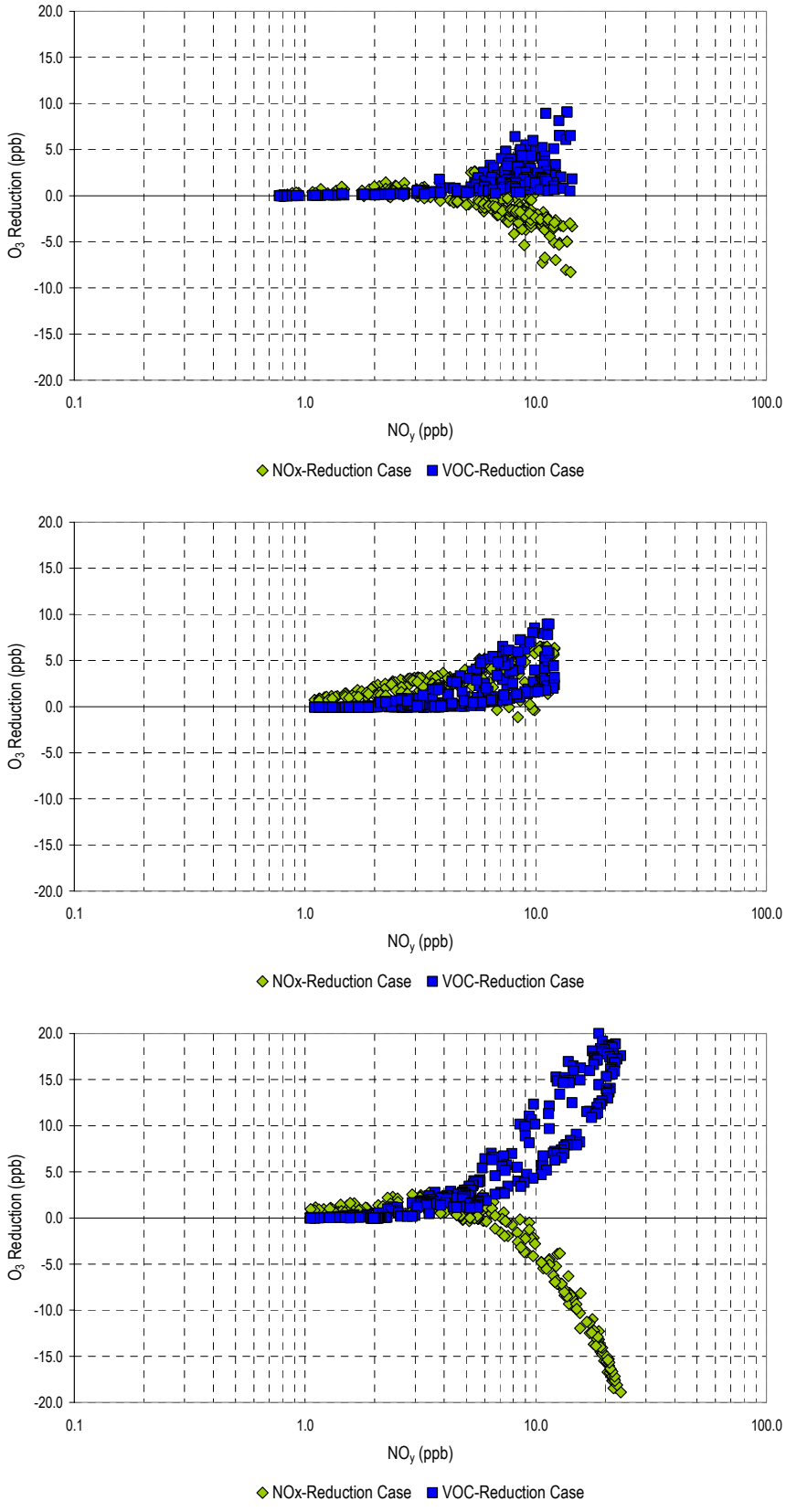

Figure 7.5. Predicted reduction in peak O_3 (in ppb) resulting from a 35% reduction in the emission rate for NO_x (diamonds) and VOCs (squares) plotted against NO_y (ppb) in the simulation for (a) Barcelona Geographical Area; (b) Plana de Vic; and (c) Alcover (1200UTC).

Reductions of VOCs in ALC yield higher O_3 reductions than in BGA. Nevertheless, results from VIC scenario (Figure 7.5b) illustrate a less successful correlation between sensitivity and NO_y. Here, the range of NO_y values associated with the transition regime is wider (Table 7.3). The difference in NO_x-VOC sensitivity between this background scenario and the urban and industrial scenarios is reflected by higher NO_y in the latter, despite NO_x- and VOC-sensitive photochemistry occurs virtually at the same NO_y in each.

NO_z. NO_z, representing the sum of NO_x reaction products (NO_y-NO_x), can also be used as an indicator for sensitivity. Generally, NO_z has a worse correlation with sensitivity than NO_y with a broader overlap between both regimes (Sillman, 1995). The indicators based on NO_y ratios can all be used for NO_z, and vice versa. Results for O_3/NO_z indicator are shown in Figure 7.6. For BGA and ALC (Figures 7.6a and 7.6c), the performance of O_3/NO_z as an indicator is comparable to NO_y with a well-defined transition between NO_x-sensitive chemistry (O_3/NO_z > 22) and VOC-sensitive chemistry (indicator values under 18). For VIC scenario (Figure 7.6b), this indicator performs much worse, as reflected in Table 7.3. Transition regime is also achieved around $O_3/NO_z \approx 20$, but the overlapping of regimes is wider, as derived from simulations. Therefore, results show a strong contrast in the performance of the indicator when evaluating sensitivity regimes between different scenarios.

HCHO and NO_y. An interesting feature of HCHO/NO_y as an indicator is that this correlation represents the impact of changes in VOCs emissions. The ratio HCHO/NO_y functions as a reactivity-weighted VOCs/NO_x ratio, since production of HCHO is roughly proportional to the summed rate of reactions of VOCs with OH. Therefore, the ratio HCHO/NO_y can also be associated with NO_x-VOCs sensitivity through the analysis of odd hydrogen. Low HCHO/NO_y is associated with VOC-sensitive ozone, a result that parallels the relation between ozone sensitivity and VOCs/NO_x (Sillman and He, 2002). The correlation between sensitivity and HCHO/NO_y is comparable with NO_y in its consistency, although its usefulness is partially compromised by its relatively narrow range of values. The model predicts the crossover between NO_x- and VOC-sensitive ozone occurs at HCHO/$NO_y \approx$ 0.6-0.7 for all domains (Figure 7.7). Results illustrate the differences between largely NO_x-sensitive chemistry in Plana de Vic scenario and VOC-sensitivity chemistry in Barcelona Geographical Area and Alcover. Nevertheless, large fractions of the model domains are associated with overlap between NO_x- and VOC-sensitive ranges (Table 7.3).

H_2O_2 and HNO_3. Representation of H_2O_2 and HNO_3 chemistry involves many complex reactions and possible unknowns that become very important under low NO_x/VOCs ratios (Kuhn *et al.*, 1998). The connection between NO_x-VOCs sensitivity and the ratio H_2O_2/HNO_3 is strong in the scenarios simulated. Nevertheless, this ratio behaves as an average indicator bearing in mind the overlap between NO_x- and VOC-sensitive regimes. This transition (Figure 7.8) takes place at a value of H_2O_2/HNO_3 of approximately 2.5-3 for the scenarios considered, being an accurate indicator in BGA and ALC (Table 7.3).

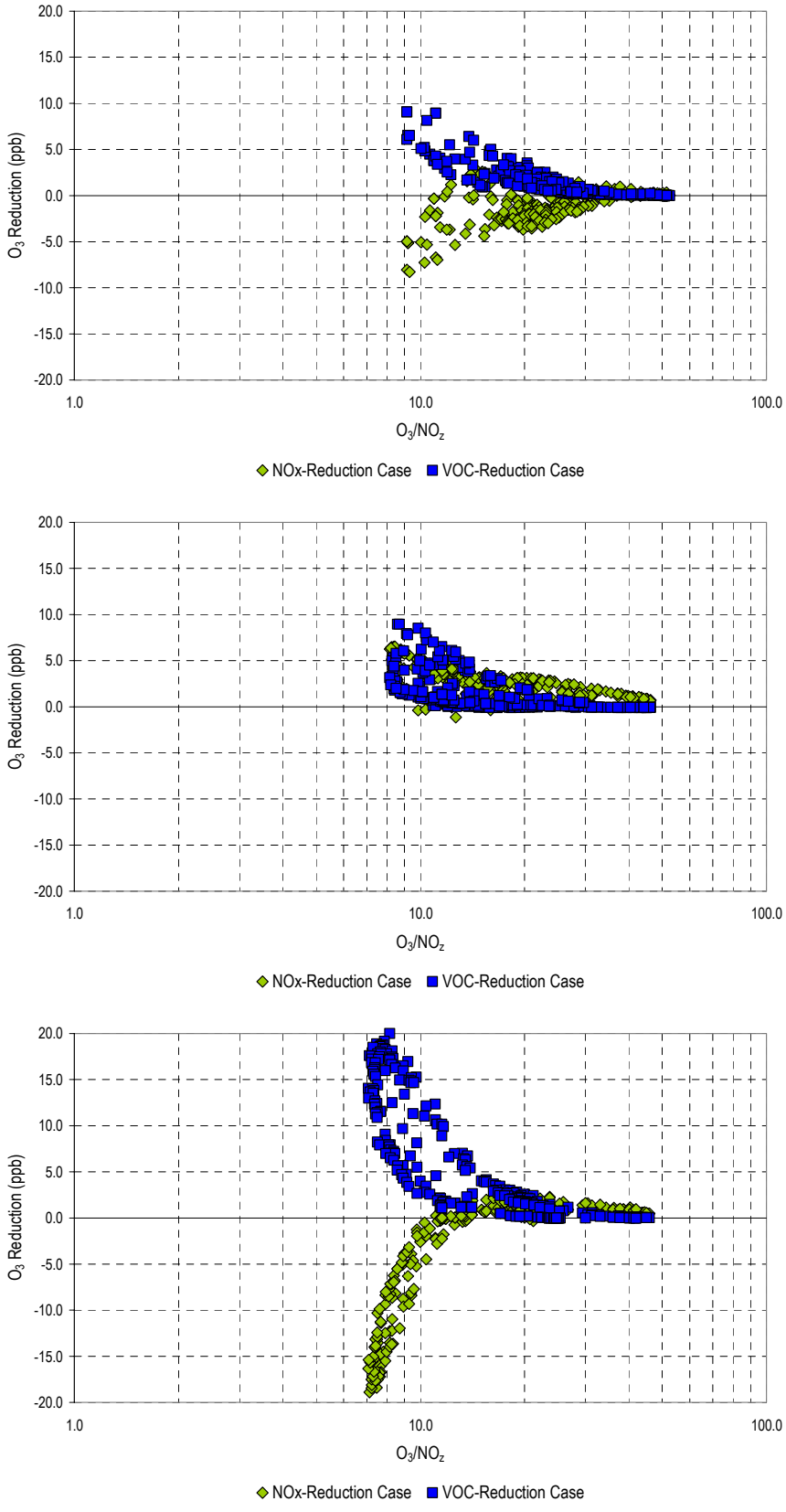

Figure 7.6. Predicted reduction in peak O_3 (in ppb) resulting from a 35% reduction in the emission rate for NO_x (diamonds) and VOCs (squares) plotted against O_3/NO_z in the simulation for (a) Barcelona Geographical Area; (b) Plana de Vic; and (c) Alcover (1200UTC).

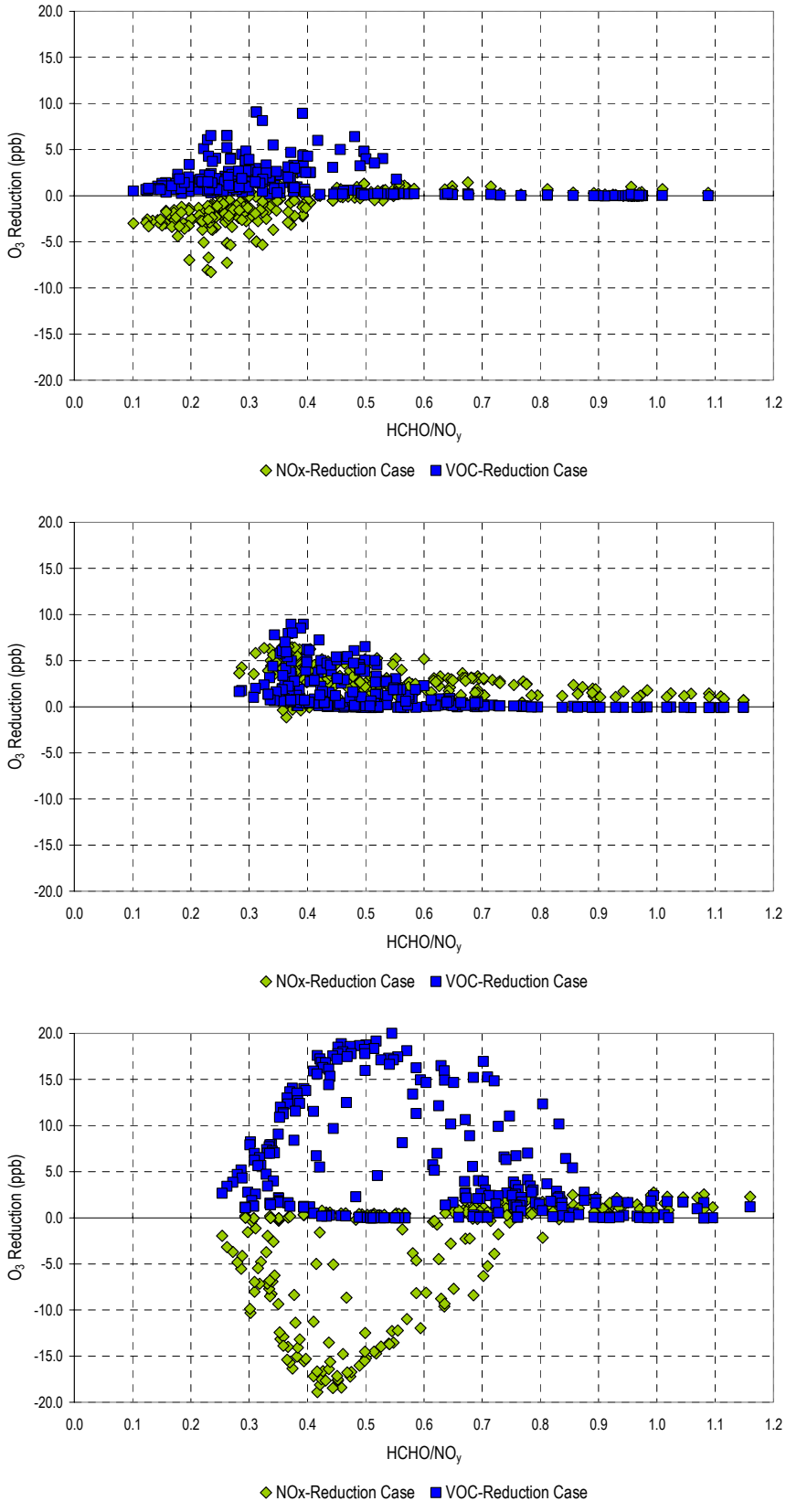

Figure 7.7. Predicted reduction in peak O_3 (in ppb) resulting from a 35% reduction in the emission rate for NO_x (diamonds) and VOCs (squares) plotted against $HCHO/NO_y$ in the simulation for (a) Barcelona Geographical Area; (b) Plana de Vic; and (c) Alcover (1200UTC).

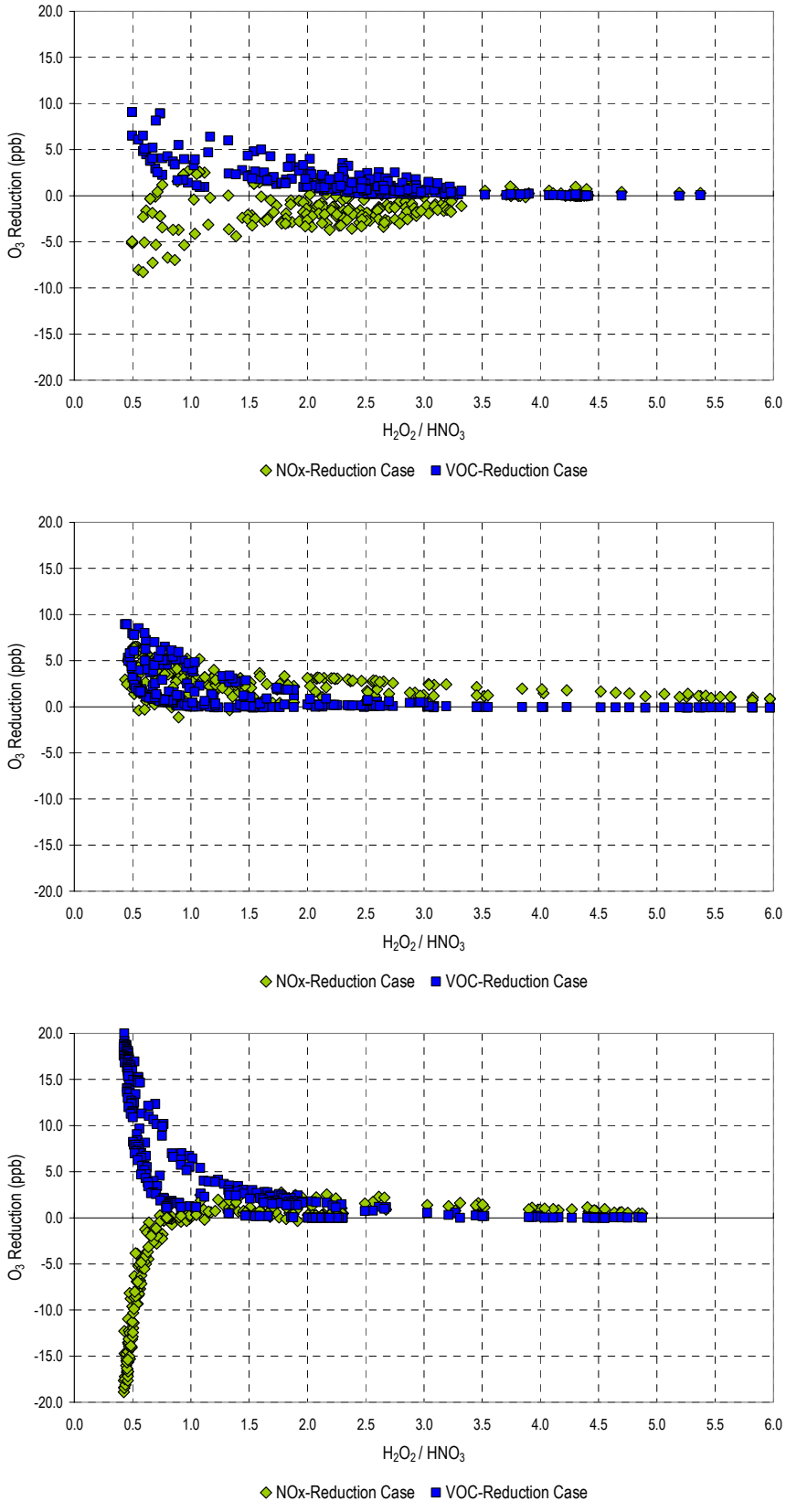

Figure 7.8. Predicted reduction in peak O_3 (in ppb) resulting from a 35% reduction in the emission rate for NO_x (diamonds) and VOCs (squares) plotted against H_2O_2/HNO_3 in the simulation for (a) Barcelona Geographical Area; (b) Plana de Vic; and (c) Alcover (1200UTC).

H_2O_2/NO_y indicator is also included in Table 7.3, showing a similar pattern, with transition values around 0.5. For H_2O_2/NO_z, its behavior strongly depends on the domain of study, being the transition value around 0.8. The lack of a relationship between H_2O_2 and HNO_3 is partially explained by their tendency to assume different correlative patterns in NO_x- versus VOC-sensitive conditions. There is no consistent correlation between the simulated H_2O_2 and HCHO or between H_2O_2 and O_3. However, there is a triple correlation among O_3, H_2O_2 and NO_x reaction products. The sum H_2O_2 + NO_z represents the cumulative sink for odd hydrogen and may be expected to correlate with O_3. As depicted in Figure 7.9, a correlation of this type is observed in all domains; the same type of relationship is observed for NO_z and HNO_3. This view, presented by Sillman (1995), emphasizes O_3 as a source for odd hydrogen, either directly or through association with intermediate hydrocarbons, and rates of formation for both peroxides and reactive nitrogen as limited by size of the odd hydrogen source. The transition from NO_x- to VOC-sensitive chemistry is linked with the replacement of peroxides by HNO_3 as the dominant sink for odd hydrogen, and therefore by a decreasing ratio of O_3 to reactive nitrogen.

Extent of Reaction. The definition of extent of reaction –EOR– (Blanchard *et al.*, 1999; Blanchard and Stoeckenius, 2001) used in this work has been modified in order be expressed as a function on NO_x and NO_y (equation 7.3):

$$\text{Extent} = \left[1 - \frac{NO_x}{1.3 \cdot NO_y}\right] \cdot 0.67 \qquad (7.3)$$

The predicted O_3 response versus EOR exhibits considerable variability and a range of indeterminate values (0.4 - 0.6); nevertheless, the delimitation of the transition between NO_x- and VOC-limitation is fairly sharp. This parameter is correlated with NO_x-VOC sensitivity. BGA is related with the lowest values of the noon EOR (under 0.35); ALC presents EOR values between 0.35 and 0.5, corresponding to primarily VOC-sensitive sites. Meanwhile VIC (where most cells are NO_x-sensitive) presents values of EOR over 0.55.

NO_x-VOCs parameter. It is also possible to develop a statistical correlation between NO_x-VOCs sensitivity and model indicator values if a single numerical value is used to express model NO_x-VOCs sensitivity. We will use the NO_x-VOCs parameter (equation 7.4) defined by Sillman *et al.* (1997):

$$NO_x - \text{VOC parameter} = \frac{[O_3]_N - [O_3]_V}{\max\{[O_3]_0; [O_3]_N; [O_3]_V\} - \min\{[O_3]_0; [O_3]_N; [O_3]_V\}} \qquad (7.4)$$

where $[O_3]_0$ represents O_3 at the specified time and location in the base case scenario, $[O_3]_N$ represents O_3 in the simulation with reduced NO_x and $[O_3]_V$ represents O_3 in the simulation with reduced VOCs.

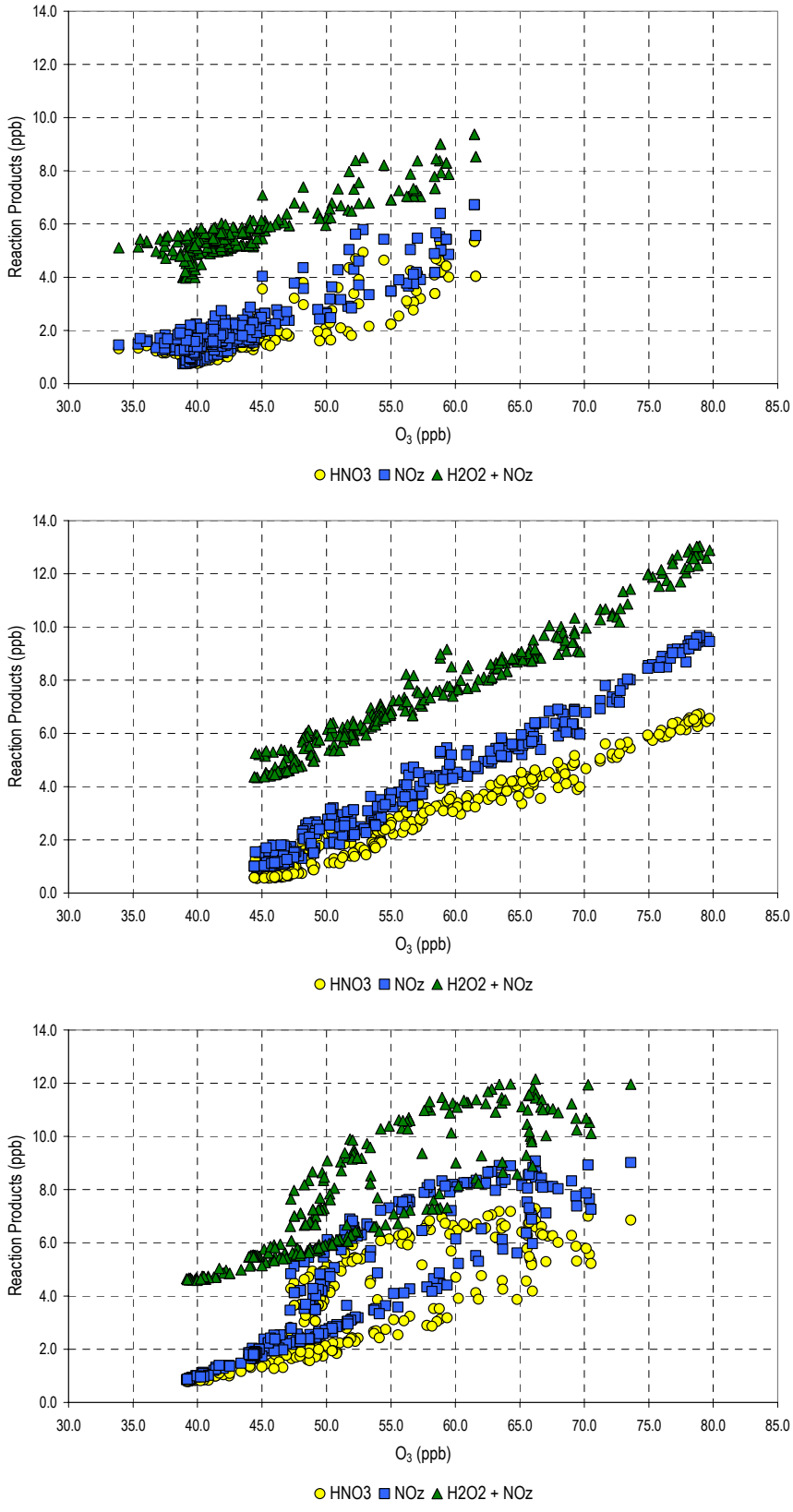

Figure 7.9. HNO_3 (circles), NO_z (squares) and H_2O_2 + NO_z (triangles) versus O_3, all in ppb, at 1200UTC in simulations for (a) Barcelona Geographical Area; (b) Plana de Vic and (c) Alcover.

The parameter is positive whenever O_3 is lower in the reduced-VOCs simulation than in the reduced-NO_x simulation. When the O_3 reduction associated with reduced VOCs is twice as large as the O_3 reduction for reduced NO_x, the parameter is 0.5; and when model NO_x reductions result in either no change or an increase in O_3, the parameter is 1. Negative values represent equivalent NO_x-sensitive results.

The quality of the NO_x-VOCs indicator correlation is demonstrated by three factors (Sillman *et al.,* 1997): (1) the size of the difference between indicator values associated with NO_x-sensitive, VOC-sensitive and transitional chemistry; (2) the lack of overlap between indicator values associated with NO_x- and VOC-sensitive locations; and (3) the consistency of the NO_x-VOCs transition value in different simulations. As seen in Table 7.3 and Figure 7.10, this parameter correlates with model values for most photochemical indicators. Correlation coefficients (r^2) of 0.50 or higher are found for all simulations and indicators. Correlation is lower for Plana de Vic since most of the domain is strongly NO_x-sensitive, and the wide range of indicator values among NO_x-sensitive locations lowers the statistical correlation.

7.4.3 Uncertainties

The use of based-model chemical relationship involves uncertainties based on model simplifications (Jiménez *et al.*, 2003). We define the uncertainty of the indicators as the fraction of the model domain with indicator values that are within 20% of the range of indicator values associated with the opposite NO_x-VOCs sensitivity. This parameter is recorded for each indicator and each domain in Table 7.3 and will help identifying their usefulness.

The extent of overlap between NO_x-sensitive and VOC-sensitive ranges for indicator species and model domains provides a partial representation of the uncertainties associated with the sensitivity-indicator correlations. The uncertainty factor is relatively higher for every indicator involving H_2O_2 and HNO_3, especially in VIC, which is mainly a NO_x-limited scenario, since of the high solubilities of these species, which makes them sensitive to surface deposition and aerosol formation rates (as stated by Sillman, 1995), which involve vague representation in photochemical models. H_2O_2 is vulnerable to reaction rate and mechanism uncertainties, so it must be considered carefully when using it as an indicator of sensitivity regime. Smallest uncertainties are achieved when using indicators related to total reactive nitrogen (NO_y or O_3/NO_y), in the order of 5% for BGA, 40% for VIC and 10% for ALC. NO_z-related indicators (NO_z, O_3/NO_z, H_2O_2/NO_z) carry a high uncertainty when used in VIC domain (NO_x-limited); nevertheless, its uncertainty decreases in VOC-limited domains as BGA or ALC. NO_z is expected to vary significantly in response to changes in radiation and production rates of odd hydrogen. The uncertainty in the relationship between extent of reaction and NO_x- or VOC-sensitive regimes is also low, since transition range is well delimited; in addition, it exhibits a good correlation with the NO_x-VOCs parameter as previously defined.

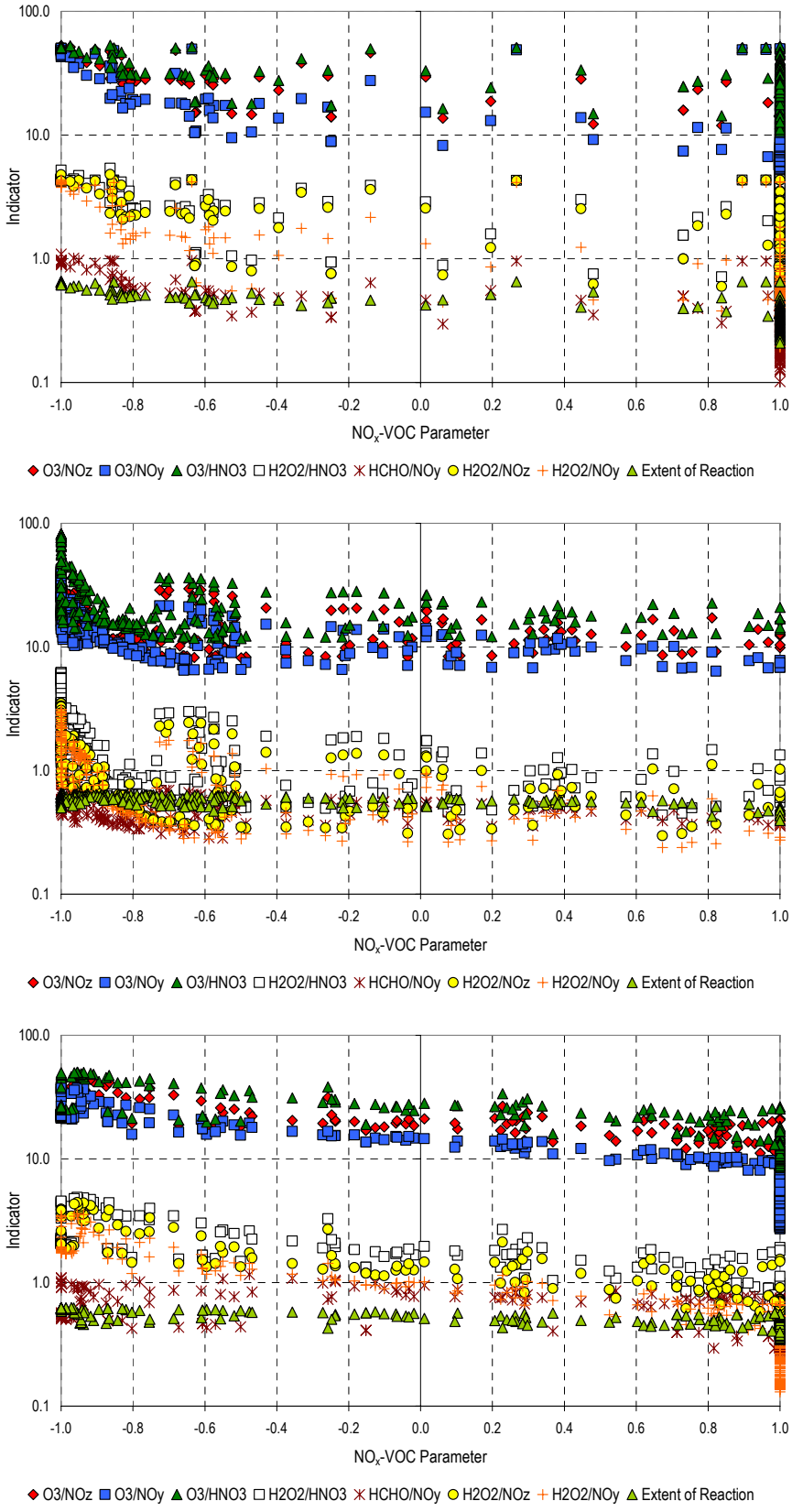

Figure 7.10. Indicators versus NO_x-VOCs parameter at 1200UTC in simulations for (a) Barcelona Geographical Area; (b) Plana de Vic; and (c) Alcover.

Table 7.3. Distribution of photochemical indicator values for NO_x- and VOC-sensitive chemistry.

Indicator	*NO_x-Sensitive Locations*				*VOC-Sensitive Locations*					
	Range	2nd Percentile	50th Percentile	98th Percentile	Range	2nd Percentile	50th Percentile	98th Percentile	Uncertainty	Correlation r^2
NO_y (ppb)										
Barcelona Area	5.24-6.60	5.26	5.44	6.60	5.95-14.16	6.08	9.06	13.68	0.07	0.73
Plana de Vic	1.98-12.06	2.37	5.74	11.69	3.83-12.06	4.34	7.66	12.02	0.41	0.53
Alcover	2.28-5.86	2.31	3.18	5.42	3.45-23.33	3.93	12.19	22.05	0.22	0.71
NO_z (ppb)										
Barcelona Area	3.67-4.17	3.68	3.78	4.17	1.88-6.72	2.00	3.17	6.61	0.05	0.32
Plana de Vic	1.69-9.68	1.88	5.15	9.55	2.65-9.68	3.00	6.35	9.60	0.49	0.40
Alcover	1.94-4.18	1.95	2.53	3.91	2.21-9.07	2.41	6.31	8.90	0.28	0.80
$HCHO/NO_y$										
Barcelona Area	0.34-0.38	0.34	0.37	0.38	0.18-0.53	0.20	0.31	0.51	0.09	0.78
Plana de Vic	0.28-0.87	0.32	0.45	0.77	0.33-0.60	0.34	0.42	0.55	0.52	0.40
Alcover	0.77-1.16	0.78	0.93	1.14	0.25-0.99	0.28	0.50	0.84	0.23	0.50
H_2O_2/NO_z										
Barcelona Area	0.76-0.91	0.76	0.86	0.91	0.39-2.03	0.40	1.09	1.95	0.05	0.55
Plana de Vic	0.30-2.03	0.32	0.64	1.81	0.30-1.28	0.31	0.48	1.09	0.47	0.44
Alcover	0.74-1.75	0.82	1.28	1.74	0.33-1.54	0.34	0.47	1.38	0.25	0.87
H_2O_2/NO_y										
Barcelona Area	0.48-0.64	0.48	0.57	0.64	0.19-0.60	0.19	0.38	0.59	0.18	0.75
Plana de Vic	0.24-1.74	0.27	0.57	1.51	0.24-0.88	0.24	0.40	0.76	0.41	0.50
Alcover	0.53-1.49	0.59	1.03	1.47	0.13-0.95	0.14	0.24	0.83	0.25	0.91
O_3/NO_z										
Barcelona Area	13.99-15.36	13.99	14.88	15.33	9.14-22.94	9.15	15.87	22.25	0.04	0.60
Plana de Vic	8.16-28.99	8.26	12.32	26.48	8.16-19.43	8.21	10.63	17.03	0.50	0.41
Alcover	13.93-23.64	14.59	19.43	23.64	7.08-21.20	7.16	8.93	20.04	0.27	0.87

Table 7.3 (continued). Distribution of photochemical indicator values for NO_x- and VOC-sensitive chemistry.

Indicator	*NO_x-Sensitive Locations*				*VOC-Sensitive Locations*					
	Range	2nd Percentile	50th Percentile	98th Percentile	Range	2nd Percentile	50th Percentile	98th Percentile	Uncertainty	Correlation r^2
O_3/NO_y										
Barcelona Area	8.85-10.76	8.85	10.45	10.73	3.13-9.17	3.47	5.64	8.15	0.02	0.75
Plana de Vic	6.45-24.84	6.57	10.79	21.59	6.35-13.43	6.54	8.83	12.51	0.38	0.50
Alcover	9.92-20.14	10.56	15.41	19.95	2.72-14.73	2.77	4.84	12.81	0.12	0.93
O_3/HNO_3										
Barcelona Area	17.29-18.75	17.29	18.09	18.73	10.70-32.09	11.14	20.88	30.84	0.04	0.57
Plana de Vic	11.72-49.40	11.93	17.18	44.33	11.72-26.39	11.78	15.27	23.20	0.59	0.39
Alcover	20.31-36.07	20.99	27.99	35.92	8.49-27.64	8.70	11.09	26.93	0.22	0.84
H_2O_2/HNO_3										
Barcelona Area	0.94-1.12	0.94	1.05	1.11	0.49-2.75	0.50	1.49	2.61	0.04	0.50
Plana de Vic	0.44-3.45	0.47	0.89	3.04	0.44-1.74	0.45	0.69	1.45	0.57	0.41
Alcover	1.08-2.66	1.17	1.84	2.65	0.42-1.92	0.43	0.56	1.80	0.18	0.85
EOR										
Barcelona Area	0.48-0.53	0.48	0.51	0.52	0.24-0.54	0.24	0.36	0.50	0.07	0.80
Plana de Vic	0.50-0.65	0.51	0.60	0.64	0.39-0.63	0.43	0.57	0.63	0.63	0.57
Alcover	0.48-0.59	0.49	0.56	0.59	0.35-0.58	0.35	0.42	0.54	0.30	0.77

Table 7.3 presents a summary of transition regimes for all indicators, as well as 2nd, 50th and 98th percentiles of indicators in NO_x- and VOC-sensitive locations for both scenarios. Results show that median values for indicators involving NO_y or NO_z species diverge in a factor of approximately 2-3 in the scenario of BGA and VIC; on the other side, no relevant difference is shown for these indicators in VIC, a domain whose cells are mainly NO_x-limited. For O_3/HNO_3 and H_2O_2/HNO_3, NO_x-sensitive locations exhibit a higher value than VOC-sensitive locations in both domains by a factor of 2. The 98th percentile of the distribution of indicator values for NO_x-sensitive locations is approximately equal than the 2nd percentile of the indicator distribution for VOC-sensitive locations in the case of NO_y, NO_z, demonstrating the robustness of the correlation between indicator values and NO_x-VOC sensitivity. Other indicators that permit us establish an accurate transition regime independently of the domain considered are $HCHO/NO_y$, O_3/NO_y, H_2O_2/HNO_3 and extent of reaction, where the 98th percentile VOC-sensitive value is of the same magnitude than the 2nd percentile NO_x-sensitive value.

7.5 Conclusions

This study has provided a case study of how the method of photochemical indicators can be used to evaluate O_3-NO_x-VOCs sensitivity in very complex terrains, showing the correlation between photochemical indicators and simulated NO_x-VOCs sensitivity in a terrain as complex as the northeastern Iberian Peninsula during a typical re-circulation episode of photochemical pollution. The model evaluation shown here is relatively simple to perform and provides a test for sensitivity evaluation and to establish control policies for ozone-precursor emissions. Nevertheless, indicators are subject to many uncertainties, including deposition rates, aerosol interactions and case-to-case variations.

Results shown suggest that O_3 chemistry in the Barcelona city plume arriving at VIC is close to the transition between VOC-sensitive and NO_x-sensitive conditions. Nevertheless, BGA and ALC present a high VOC-sensitive behavior due to the high traffic and industrial NO_x emissions. Predicted NO_x-VOCs sensitivity varies considerably among the three model scenarios. NO_x-sensitive chemistry is associated with lower O_3 and NO_y; the varying NO_x-VOCs predictions occur despite O_3 is similar in all three scenarios.

Variations in indicator behavior are analytically linked to variations in the O_3 production efficiency per primary radical production. In general, H_2O_2- and HNO_3- derived indicators entail higher uncertainties since transition regimes between NO_x and VOCs sensitivity cover a wide range, because those indicators (and their ratio) are affected by changes in environmental conditions. NO_y and O_3/NO_y are revealed as the most accurate indicators to assess sensitivity in the domains studied, attending to the narrow transition regime between NO_x- and VOC-sensitive chemistry and the low uncertainty observed; on the other side, NO_z-indicators correlates worse than NO_y and implies a higher uncertainty. The behavior of NO_z tends to disagree for differently polluted

domains; hence, it performs better in VOC-sensitive (BGA, a metropolitan area; or ALC, an industrial zone characterized by high NO_x and VOC emissions) than in NO_x-sensitive scenarios as VIC. The extent of reaction also performs as a good indicator to separate NO_x and VOCs sensitive regimes. The results given in this study indicate the necessity to consider the differences in the conditions of the domains when applying the indicator approach.

The biggest weakness of these indicators is the difficulty in testing the predicted indicator-NO_x-VOCs relationship against ambient measurements. In addition, the indicator method provides information about NO_x-VOCs sensitivity at the time and place considered. NO_x-VOCs sensitivity varies with time of day, changes from event to event, and by location within a same domain.

7.6 References

Atkinson, R., 2000. Atmospheric chemistry of VOCs and NO_x. Atmospheric Environment, **34**, 2063-2101.

Andreani-Aksoyoglu, S., Lu, C.-H., Keller, J. Prévôt, A.S.H., Chang, J.S., 2001. Variability of indicator values for ozone production sensitivity: a model study in Switzerland and San Joaquin Valley (California). Atmospheric Environment, **35**, 5593-5604.

Blanchard, C.L., Lurmann, F.W., Roth, P.M., Jeffries, H.E., Korc, M., 1999. The use of ambient data to corroborate analyses of ozone control strategies. Atmospheric Environment, **33**, 369-381.

Blanchard, C.L., Fairley, D., 2001. Spatial mapping of VOC and NO_x-limitation of ozone formation in central California. Atmospheric Environment, **35**, 3861-3873.

Blanchard, C.L., Stoeckenius, T., 2001. Ozone response to precursor controls: comparison of analysis methods with the predictions of photochemical air quality simulation models. Atmospheric Environment, **35**, 1203-1215.

Hogrefe, C., Rao, S.T., Kasibhatla, P., Hao, W., Sistla, G., Mathur, R., McHenry, J., 2001. Evaluating the performance of regional-scale photochemical modeling systems: Part II – ozone predictions. Atmospheric Environment, **35**, 4175-4188.

Jiménez, P., Dabdub, D., Baldasano, J.M., 2003. Comparison of photochemical mechanisms for air quality modeling. Atmospheric Environment, **37**, 4179-4194.

Kleinman, L.I., Daum, P.H., Lee, J.H., Lee, Y.-N., Nunnermacjerm L.J. Springston, S.R., Newman, L., Weinstein-Lloyd, J., Sillman, S., 1997. Dependence of ozone production on NO_x and hydrocarbons in the troposphere. Geophysical Research Letters, **24**, 2299-2302.

Kuhn, M., Builtjes, P.J.H., Poppe, D., Simpson, D., Stockwell, W.R., Andersson-Skold, Y., Baart, A., Das, M., Fiedler, F., Hov, O., Kirchner, F., Makar, P.A., Milford, J.B., Roemer, M.G.M., Ruhnke, R., Strand, A., Vogel, B., Vogel, H., 1998. Intercomparison of the gas-phase chemistry in several chemistry and transport models. Atmospheric Environment, **32**, 693-709.

Lu, C.-H., Chang, J., 1998. On the indicator-based approach to assess ozone sensitivities and emission features. Journal of Geophysical Research, **103**, 3453-3462.

Milford, J.B., Gao, D., Sillman, S., Blossey, P., Russell, A.G., 1994. Total reactive nitrogen (NO_y) as an indicator of the sensitivity of ozone to reductions in hydrocarbon and NOx emissions. Journal of Geophysical Research, **99** (D2), 3533-3542.

Russell, A., Dennis, R., 2000. NARSTO critical review of photochemical models and modeling. Atmospheric Environment, **34**, 2283-2324.

Sillman, S., 1995. The use of NO_y, H_2O_2 and HNO_3 as indicators for ozone-NO_x-hydrocarbon sensitivity in urban locations. Journal of Geophysical Research, **100** (D7), 14175-14188.

Sillman, S., He, D., Cardelino, C., Imhoff, R.E., 1997. The use of photochemical indicators to evaluate ozone-NO_x-hydrocarbon sensitivity: case studies from Atlanta, New York and Los Angeles. Journal of the Air & Waste Management Association, **47**, 1030-1040.

Sillman, S., He, D., Pippin, M.R., Daum, P.H., Imre, D.G., Kleinman, L.I., Lee, J.H., Weinstein-Lloyd, J., 1998. Model correlations for ozone, reactive nitrogen and peroxides for Nashville in comparison with measurements: implications for VOC-NO_x sensitivity. Journal of Geophysical Research, **103**, 22629 - 22644.

Sillman, S., 1999. The relation between ozone, NO_x and hydrocarbons in urban and polluted rural environments. Atmospheric Environment, **33**, 1821-1845.

Sillman, S., He, D., 2002. Some theoretical results concerning O_3-NO_x-VOC chemistry and NOx-VOC indicators. Journal of Geophysical Research, **107** (D22), 4659, doi:10.1029/2001JD001123, 2002.

Sillman, S., Vautard, R. Menut, L., Kley, D., 2003. O_3-NO_x-VOC sensitivity and NO_x-VOC indicators in Paris: results from models and atmospheric pollution over the Paris area (ESQUIF) measurements. Journal of Geophysical Research, **108** (D17), 8563, doi:10.1029/2002JD001561, 2003.

Tonnesen, G.S., Dennis, R.L., 2000a. Analysis of radical propagation efficiency to assess ozone sensitivity to hydrocarbons and NO_x, 1, Local indicators of instantaneous odd oxygen production sensitivity. Journal of Geophysical Research, **105**, 9213-9226.

Tonnesen, G.S., Dennis, R.L., 2000b. Analysis of radical propagation efficiency to assess ozone sensitivity to hydrocarbons and NO_x, 2, Long-lived species as indicators of ozone concentration sensitivity. Journal of Geophysical Research, **105**, 9227-9242.

US EPA, 1991. Guideline for Regulatory Application of the Urban Airshed Model. US EPA Report No. EPA-450/4-91-013. Office of Air and Radiation, Office of Air Quality Planning and Standards, Technical Support Division. Research Triangle Park, North Carolina, US.